CHEMISTRY OF MATERIALS

Communication

pubs.acs.org/cm

Efficient, Low Cost Synthesis of Sodium Platinum Bronze $Na_xPt_3O_4$

David Horwat,[†,‡,*] Moukrane Dehmas,[†,‡] Alejandro Gutiérrez,[§] Jean-François Pierson,[†,‡] André Anders,[∥] Flavio Soldera,[⊥] and José-Luis Endrino[#]

[†]Institut Jean Lamour, Université de Lorraine, UMR 7198, Nancy, F-54000, France

[‡]CNRS, Institut Jean Lamour, UMR 7198, Nancy, F-54000, France

[§]Departamento de Física Aplicada and Instituto Nicolás Cabrera, Universidad Autónoma de Madrid, Cantoblanco, 28049 Madrid, Spain

[∥]Lawrence Berkeley National Laboratory, University of California, 1 Cyclotron Road, Berkeley, California 94720, United States

[⊥]Functional Materials, Saarland University, P.O. Box 151150, D-66041 Saarbrücken, Germany

[#]Abengoa Research, Campus Palmas Altas, E-41014 Sevilla, Spain

Supporting Information

KEYWORDS: *thin films, platinum, oxide, soft synthesis, sodium*

Noble metal oxide surfaces with metals of the platinum group are of prime importance for catalytic reactions such as the reduction of nitrogen oxides[1] and the catalytic combustion of methane.[2] Pt_3O_4 is theoretically highly efficient for the conversion of methane[3] but is stable only in a narrow range of temperatures around 900 K. To overcome that problem, solid solutions of Pt_3O_4 and sodium can be stabilized in $Na_xPt_3O_4$ compounds with $0 < x < 1$. The ternary compound is one of the most intriguing oxides with a unique combination of peculiar physical and chemical properties such as a bifunctional catalytic behavior, electronic conductivity, and mixed valency. Its study remains difficult due to very small amounts of the material produced by extremely severe conditions of synthesis. We present a simple and easily upscalable way to synthesize large quantities of $Na_xPt_3O_4$. So far $Na_xPt_3O_4$ was formed only under very high pressure,[4] but we show here that it can be produced with a purity higher than 95% by deposition of platinum oxides (PtO_y) on a Na^+ conductor such as soda lime glass followed by annealing in air at atmospheric pressure. While PtO_y films deposited on silicon further oxidize if annealed in air at 300 °C and then decompose to Pt and O_2 above 500 °C, PtO_y films deposited on soda lime glass (SLG) can incorporate sodium from the substrate and only partially decompose when annealed up to about 550 °C. Above that temperature, the reduction is limited and high yields of $Na_xPt_3O_4$ can be produced.

Platinum is often qualified as a noble metal from the chemical viewpoint, but it has been known for a long time to react to form oxides.[5] In the early period the difficulties to synthesize and characterize platinum oxide compounds led to many controversies about the existence and structure of PtO, PtO_2, Pt_3O_4, and Pt_3O_8 phases owing to their poor crystallinity (a review of early works can be found in the paper of Muller and Roy[6]). Most influential was the discovery and definition of the crystalline structure of the first platinum bronze $Na_xPt_3O_4$, $0 \leq x \leq 1$, by Wäser and McClanahan in 1951.[7] The cubic "$NaPt_3O_4$ structure" or Waserite is an archetype structure which turned out to be ubiquitous in ternary platinum and palladium oxides containing alkali (Li, K), alkaline earth (Mg, Ca, Ba), and transition metals (Co, Ni, Zn, Cu, Cd, Pt) as an electron donor counterion.[8] $Na_xPt_3O_4$ crystallizes in the Pm_3n space group and is a solid solution of Na in Pt_3O_4. Its discovery motivated many studies until the early 1980s due to a unique combination of metallic conductivity,[9] nonstoichiometry, good catalytic activity, and chemical stability (even in boiling aqua regia[8b]). Catalytic applications of $Na_xPt_3O_4$ were the most promising owing to its high efficiency for the electrolytic production of chlorine and caustic soda[10] and to a bifunctional behavior when used as oxygen electrodes for rechargeable alkaline fuel cells.[11] It is also active for hydrogenating organic compounds and is supposed to be the main active component of the Adams catalyst.[12] Later on, the interests for $Na_xPt_3O_4$ vanished due to restrictive conditions of synthesis.

To the best of our knowledge, the hydrothermal synthesis is the only known route to produce $Na_xPt_3O_4$ of good purity. It consists in heating a mixture of PtO_2, NaOH, $KClO_3$, and H_2O in a platinum crucible for about a day close to 1000 K and under 3000 atm of oxygen.[4] The amount of sodium platinum bronze produced this way is very small (typically few milligrams).

Physical vapor deposition methods allow condensing a metal vapor on a surface near room temperature in a reactive atmosphere to synthesize metal compounds far from thermodynamics equilibrium. Hence, amorphous platinum oxide PtO_y films can be formed by reactive magnetron sputtering of a platinum target in an oxygen-containing atmosphere.[13] In the absence of a reaction with the surrounding medium, PtO_y films readily thermally decompose into metal platinum and molecular gaseous oxygen around 500 °C. Pt_3O_4

Received: April 17, 2012
Revised: June 21, 2012
Published: June 25, 2012

   dx.doi.org/10.1021/cm301179x | *Chem. Mater.* 2012, 24, 2429−2432

can be detected in very small amounts in the films as an intermediate product.

The nature of the substrate has been shown to have a sensitive impact on the growth and evolution of compounds in thin film form.[14] The thermal decomposition of PtO_y films is likely to strongly modify film−substrate interactions, more particularly if an element of the substrate is mobile. The latter is particularly true with ion conducting substrates.

We have deposited PtO_y films on silicon and SLG slides (Menzel Gläzer, 10 atom % Na). Chemical and structural evolutions of the films upon annealing in air were probed by X-ray absorption near edge structure (XANES) at the Pt-L_3 edge, X-ray diffraction (XRD), and high resolution transmission electron microscopy (HRTEM). Figure 1a displays the evolution of the electronic structure of PtO_y films deposited on silicon and SLG during annealing for two hours in air, as probed by Pt-L_3 total fluorescence yield X-ray absorption spectroscopy. The region which extends from a few eV before the main inflection point (absorption threshold at 11550 eV) to about 20 eV above and corrersponding to the XANES signal is assigned to the density of empty $5d_{3/2}$ and $5d_{5/2}$ states.[15] The region starting from about 25 eV above the absorption threshold is dominated by extended X-ray absorption fine structure (EXAFS) oscillations and is very sensitive to the symmetry of the films. The evolution of the electronic structure upon annealing and comparison with the structure of a platinum foil illustrates that the film deposited on silicon decomposes into metallic platinum and oxygen between 500 and 550 °C, which is in line with previous studies.[13] Using XRD we verified the appearance of diffraction lines of fcc platinum when annealing in air above 500 °C. In contrast, the films deposited on SLG progressively transform into a different compound. In oxidized platinum, a transfer of 5d electrons from platinum to oxygen occurs, leading to emptying of the 5d states and rising of the resonance located at 11559−11562 eV. Following the procedure described in ref 15, the area of the resonance is exploited to determine the average oxidation state of platinum for each annealing condition. The evolution upon annealing is shown in Figure 1b (see Supporting Information Section II).

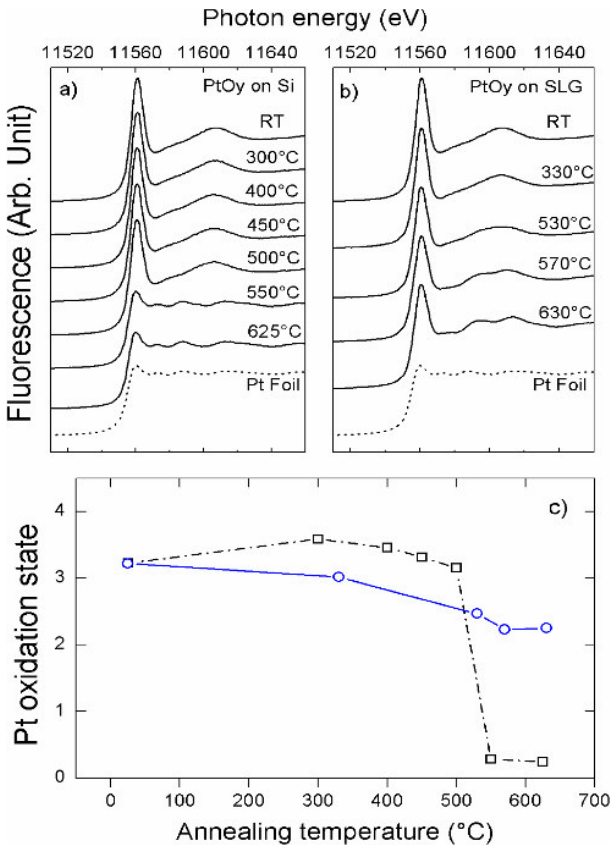

Figure 1. Pt-L_3 edge X-ray absorption near edge structure of platinum oxide thin films deposited on silicon (a), on soda lime glass (b), and annealed in air at various temperatures; corresponding oxidation states of platinum (c).

An average oxidation state of 3.2 is derived from the XANES signal of the as-deposited films, corresponding to stoichiometry $PtO_{1.6}$. This reflects the fact that sputter-deposited PtO_y films are mixtures of PtO and PtO_2 phases at the nanometer scale, as we showed recently.[16] Hence, the as-deposited films are mixtures of approximately 60 mol % PtO_2 and 40 mol % PtO. Thus, platinum is present as Pt(II) and Pt(IV). When using a silicon substrate, further oxidation of the film is observed up to an average oxidation state of 3.6 upon annealing at 300 °C, corresponding to a mixture of 80 mol % PtO_2 and 20 mol % PtO. XRD analyses indicated that the film remained nanocrystalline during the process. Annealing to 400 °C or higher promotes the decomposition of the oxide phases, with a strong acceleration above 500 °C. Decomposition is nearly complete after annealing at 550 °C .

In contrast, when using a SLG substrate, there is no further oxidation after low temperature annealing, and progressive partial reduction proceeds upon annealing up to 570 °C without leading to Pt(0). Meanwhile, the well adherent films change from transparent brownish to fully absorbent dark instead of showing the characteristic metallic reflection of Pt(0). This reveals a strong chemical interaction of the film with the substrate. An average oxidation state of 2.25 is then obtained, which is close to 2.33 for $NaPt_3O_4$. This state is maintained after annealing at 630 °C. Significant film stress is observed as evident by bending of the SLG slides at this temperature. The X-ray diffractogramms of Figure 2 show that though reduction has started, the nanocrystalline character was

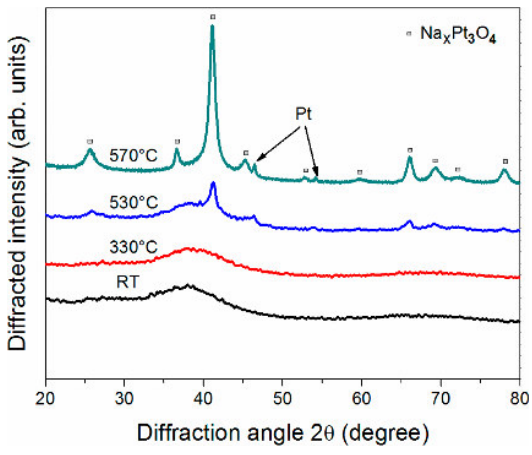

Figure 2. X-ray diffractogramms of PtO_x films as-deposited on SLG and air annealed at different temperatures. Open squares indicate the diffraction lines of $Na_xPt_3O_4$.

dx.doi.org/10.1021/cm301179x | *Chem. Mater.* 2012, 24, 2429−2432

kept after treatment at 330 °C. In contrast to the situation when using a silicon substrate, progressive growth of $Na_xPt_3O_4$ is observed from 530 to 570 °C. The signature of crystalline metallic platinum is also found from 530 °C, but its magnitude does not significantly evolve as $Na_xPt_3O_4$ forms.

Rietveld refinements (see Supporting Information Section III) indicated a cell parameter of 5.674 Å, equivalent to that of $Na_{0.73}Pt_3O_4$,[4] and evaluate the amount of platinum to 3 mol %. Indeed, few platinum crystals of about 20 nm in diameter were observed by HRTEM near the SLG−film interface. There was no evidence of another crystalline phase in the film. Moreover, Raman scattering analyses prooved the vibrational signature of the $Na_xPt_3O_4$ structure (see Supporting Information Section III). HRTEM analyses (Figure 3) provide a better insight into

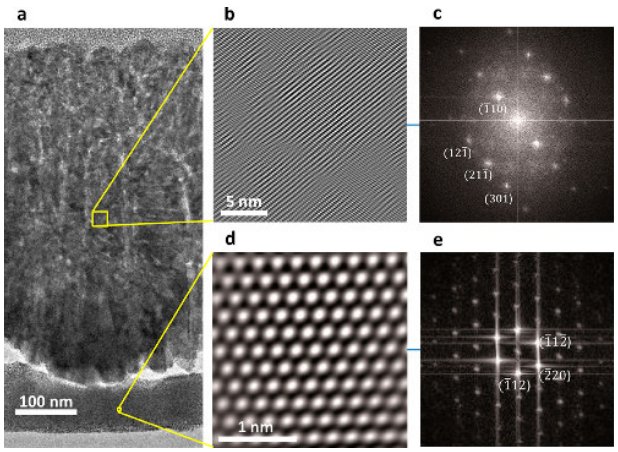

Figure 3. Cross section scanning transmission electron microscopy picture of a $PtO_{1.8}$ film deposited on SLG and annealed at 570 °C as observed by HRTEM (a). Local structures of the top (b) and bottom (d) zones and correponding electron diffraction patterns (c, e).

the local microstructure. The general view of the sample cross section of a $PtO_{1.6}$ film deposited on SLG and annealed at 570 °C provides evidence of two distinct zones. Agglomerated, randomly packed nanoparticles of approximately 2 nm in diameter, organized in an irregular layer of 70−100 nm, are in contact with SLG (Figure 3d). The film was stable during analysis.

Energy dispersive X-ray spectroscopy (EDX) measurements stated a Na/Pt atomic ratio close to 1.5 in this region, which is far above the ratio in $Na_1Pt_3O_4$. However, the particles exhibit the atomic arrangements and electron diffraction spectra of $Na_xPt_3O_4$ as shown in Figure 3d,e. The excess of sodium must therefore be segregated in the grain boundaries, thus explaining the nanocrystalline character of this region of the film. The analysis of 100 nm thick films treated in the same conditions led to the same conclusions. Very fine nanocrystalline $Na_xPt_3O_4$ can thus be formed if needed for a specific application. Just above the interface region with SLG, a 500 nm thick top zone extends up to the film surface. Secondary ion mass spectroscopy (SIMS) and EDX measurements (see Supporting Information Section II) indicate that the Na/Pt ratio is progressively decreasing with increasing distance from the film/substrate interface, down to nearly 0.6 at the film surface. The $Na_xPt_3O_4$ structure is retained in the top zone (Figure 3b,c) but with a longer crystalline coherence than in the bottom layer. The average diameter of the coherence domains has been estimated to be approximately 20 nm, which is consistent with the grain size estimated from XRD. These domains are monocrystals exhibiting few defects (dislocations) and nanostrains (Figure 3b). Neighboring domains have different orientations and are separated by disordered boundaries.

The conductivity of Na^+ ions in SLG is approximately 10^{-8} S cm^{-1} at 570 °C,[17] making SLG an efficient source of sodium. In the case of the hydrothermal synthesis,[4] a narrow range of reaction temperatures and extreme pressures are necessary to decompose the reactants producing $Na_xPt_3O_4$. With the present process, sodium is released from the SLG into the platinum oxide films, thereby facilitating the reduction of platinum to an appropriate oxidation state to form $Na_xPt_3O_4$. Thereby, films of graded composition are formed. For catalytic applications, mostly the surface composition is important, which can be set through the control of the $Na_xPt_3O_4$ film thickness. Because sputtering of PtO_y can be easily scaled up and the overall treatment used in this study is soft and cost-efficient, very large surface areas of SLG (or other Na ion conductors) functionalized with $Na_xPt_3O_4$ could be produced.

■ ASSOCIATED CONTENT

Supporting Information

Experimental details, extraction of averaged platinum oxidation state, Rietveld refinement, Raman analysis, SIMS, and EDS measurements. This material is available free of charge via the Internet at http://pubs.acs.org.

■ AUTHOR INFORMATION

Corresponding Author

*E-mail: david.horwat@ijl.nancy-universite.fr.

Notes

The authors declare no competing financial interest.

■ ACKNOWLEDGMENTS

The synchrotron work at BESSY-II was supported by the EC "Research Infrastructure Action" under the FP6 "Structuring the European Research Area Programme" through the "Integrated Infrastructure Initiative Integrating Activity on Synchrotron and Free Electron Laser Science" (Contract No. R II 3-CT-2004-506008). A.A. acknowledges support by U.S. Department of Energy under Contract No. DE-AC02-05CH11231. F.S. thanks the EFRE Funds of the European Commission for support of activities within the AME-Lab project.

■ REFERENCES

(1) Fritz, A.; Pitchon, V. *Appl. Catal., B* **1997**, *13*, 1.
(2) (a) Dallabeta, R. A.; Rostrup-Nielsen, T. *Catal Today* **1999**, *47*, 369. (b) Horwat, D.; Endrino, J. L.; Boreave, A.; Karoum, R.; Pierson, J. F.; Weber, S.; Anders, A.; Vernoux, Ph. *Catal. Commun.* **2009**, *10*, 1410.
(3) Seriani, N.; Pompe, W.; Colombi Ciacchi, L. *J. Phys. Chem. B* **2006**, *110*, 14860.
(4) (a) Schwartz, K. B.; Prewitt, C. T.; Shannon, R. D.; Corliss, L. M.; Hastings, J. M.; Chamberland, B. L. *Acta Crystallogr., Sect. B: Struct. Sci.* **1982**, *38*, 363. (b) Shannon, R. D.; Grier, T. E.; Carcia, P. F.; Bierstedt, P. E.; Flippen, R. B.; Vega, A. J. *Inorg. Chem.* **1982**, *21*, 3372.
(5) (a) Jörgensen, S. M. *J. Prakt. Chem.* **1877**, *16*, 342. (b) Wöhler, L. *Z. Anorg. Allg. Chem.* **1904**, *40*, 423. (c) Statton, W. O. *J. Chem. Phys.* **1951**, *19*, 33. (d) Van Arkel, A. E.; Flood, E. A.; Bright, N. F. H. *Can. J. Chem.* **1953**, *31*, 1009.
(6) Muller, O.; Roy, R. *J. Less-Common Met.* **1968**, *16*, 129.
(7) Wäser, J.; McClanahan, E. D. *J. Chem. Phys.* **1951**, *19*, 413.

(8) (a) Cahen, D.; Ibers, J. A.; Shannon, R. D. *Inorg. Chem.* **1972**, *11*, 2311. (b) Cahen, D.; Ibers, J. A.; Wagner, J. B. *Inorg. Chem.* **1974**, *13*, 1377.
(9) (a) Schwartz, K. B.; Prewitt, C. T.; Shannon, R. D.; Corliss, L. M.; Hastings, J. M.; Chamberland, B. L. *Acta Crystallogr., Sect. B: Struct. Sci.* **1982**, *38*, 363. (b) Robin, M.; Day, P. *Adv. Inorg. Chem. Radiochem.* **1967**, *10*, 247. (c) Doublet, M. L.; Canadell, E.; Whangbo, M. H. *J. Am. Chem. Soc.* **1994**, *116*, 2115.
(10) (a) Thiel, G.; Zollner, D.; Koziol, K. G.B. Patent 1328270, 1973. (b) Zollner, D.; Zollner, C.; Koziol, K. U.S. Patent 3962068, 1976. (c) Koziol, K.; Sieberer, K. H.; Rathjen, H. C. U.S. Patent 3948752, 1976. (d) Thiel, G.; Zollner, D.; Koziol, K. U.S. Patent 4042484, 1977.
(11) (a) Swette, L.; Giner, J. *J. Power Sources* **1988**, *22*, 399. (b) Swette, L; Kackley, N.; McCarthy, S. A. *J. Power Sources* **1991**, *22*, 323.
(12) Cahen, D.; Ibers, J. A. *J. Catal.* **1973**, *31*, 369.
(13) (a) Saenger, K. L.; Cabral, C., Jr.; Lavoie, C.; Rossnagel, S. M. *J. Appl. Phys.* **1999**, *86*, 6084. (b) Hecq, M.; Hecq, A.; Delrue, J. P.; Robert, T. *J. Less-Common Met.* **1979**, *64*, P25.
(14) (a) Brune, H. *Surf. Sci. Rep.* **1998**, *31*, 125. (b) Vlakhov, E. S.; Chakalov, R. A.; Chakalova, R. I.; Nenkov, K. A.; Dörr, K.; Handstein, A.; Müller, K. H. *J. Appl. Phys.* **1998**, *83*, 2152.
(15) (a) Lytle, F. W. *J. Catal.* **1976**, *43*, 376379. (b) Hlil, E. K.; Baudoing-Savois, R.; Moraweck, B.; Renouprez, A. J. *J. Phys. Chem.* **1996**, *100*, 3102.
(16) Mosquera, A.; Horwat, D.; Vasquez, L.; Gutierrez, A.; Erko, A.; Anders, A.; Andersson, J.; Endrino, J. L. *J. Mater. Res.* **2012**, 27.
(17) Natrup, F. V.; Bracht, H.; Murugavel, S.; Roling, B. *Phys. Chem. Chem. Phys.* **2005**, *7*, 2279.